Journal of Clinical and Translational Hepatology **2022**
DOI: 10.14218/JCTH.2021.00560

Original Article

Gasdermin D Inhibitor Necrosulfonamide Alleviates Lipopolysaccharide/D-galactosamine-induced Acute Liver Failure in Mice

Yi-Long Wu[1], Wei-Jie Ou[2], Ming Zhong[3,4], Su Lin[2,5*] and Yue-Yong Zhu[2,5*]

[1]Endoscopy Center, the First Affiliated Hospital, Fujian Medical University, Fuzhou, Fujian, China; [2]Department of Hepatology, Hepatology Research Institute, the First Affiliated Hospital, Fujian Medical University, Fuzhou, Fujian, China; [3]Endocrinology Department, Metabolic Diseases Research Institute, the First Affiliated Hospital, Fujian Medical University, Fuzhou, Fujian, China; [4]Fujian Diabetes Research Institute, the First Affiliated Hospital, Fujian Medical University, Fuzhou, Fujian, China; [5]Clinical Research Center for Liver and Intestinal Diseases of Fujian Province, Fuzhou, Fujian, China

Received: 13 December 2021 | **Revised:** 27 January 2022 | **Accepted:** 12 February 2022 | **Published:** 8 March, 2022

Abstract

Background and Aims: Acute liver failure (ALF) is associated with high mortality. Gasdermin D (GSDMD) is the executioner of pyroptosis and is involved in the pathophysiology of immune dysregulation This study investigated the role of the GSDMD inhibitor necrosulfonamide (NSA) in ALF. ***Methods:*** An ALF model was established by lipopolysaccharide/D-galactosamine challenge in C57BL/6J mice. Mice were divided into four groups: normal controls (control group), ALF group (ALF group), dimethyl sulfoxide group (DMSO group), and NSA intervention group (NSA group). Survival was monitored, liver damage was determined by hematoxylin and eosin staining, and serum alanine aminotransferase (ALT). Underlying mechanisms were explored by quantitative real-time PCR, western blotting, and enzyme-linked immunosorbent assays. ***Results:*** Pyroptosis was activated in ALF model mice. Mice treated with GSDMD inhibitor NSA developed less severe liver failure. NSA reduced the expression of GSDMD, NLRP3, cleaved caspase-1, cleaved caspase-11, and secretion of interleukin-1 beta in ALF mice model. ***Conclusions:*** Pyroptosis was activated in ALF. NSA alleviated ALF via the pyroptosis pathway.

Citation of this article: Wu Y-L, Ou W-J, Zhong M, Lin S, Zhu Y-Y. Gasdermin D Inhibitor Necrosulfonamide Alleviates Lipopolysaccharide/D-galactosamine-induced Acute Liver Failure in Mice. J Clin Transl Hepatol 2022. doi: 10.14218/JCTH.2021.00560.

Keywords: Liver failure, Acute; Pyroptosis; GSDMD; GSDMD-NT; Necrosulfonamide.

Abbreviations: ALF, acute liver failure; ALT, alanine aminotransferase; BCA, bicinchoninic acid; DAMPs, damage-associated molecular patterns; DMSO, dimethyl sulfoxide; ELISA, enzyme-linked immunosorbent; GSDMD, Gasdermin D; HE, hematoxylin-eosin staining; IL-18, interleukin-18; IL-1β, interleukin-1 beta; MLKL, mixed lineage kinase domain-like; NSA, necrosulfonamide; PVDF, polyvinylidene difluoride; qRT-PCR, quantitative real-time polymerase chain reaction.

[*]**Correspondence to:** Yue-Yong Zhu and Su Lin, Department of Hepatology, Hepatology Research Institute, the First Affiliated Hospital, Fujian Medical University; Clinical Research Center for Liver and Intestinal Diseases of Fujian Province, Fuzhou, Fujian 350005, China. ORCID: https://orcid.org/0000-0002-0746-4911 (YYZ), https://orcid.org/0000-0001-7517-9859 (SL). Tel: +86-591-87981658, Fax: +86-591-87981660, E-mail: zhuyueyong@fjmu.edu.cn (YYZ), sumer5129@fjmu.edu.cn (SL)

Introduction

Acute liver failure (ALF) is a severe liver injury,[1] there is a lack of effective treatment, and the condition has extremely high short-term mortality.[2] Twenty-one-day mortality of ALF patients is as high as 50%.[3] In-depth characterization of the pathogenesis of ALF and early intervention are of great significance for improving prognosis.

The core events in ALF are massive death of liver cells, uncontrollable intrahepatic inflammation, and systemic inflammation.[4] Release of a large number of pro-inflammatory cytokines in ALF leads to systemic inflammatory response syndrome.[5] Pyroptosis is a newly discovered type of pro-inflammatory programmed cell death.[6–9] The canonical pathway of pyroptosis is mediated by inflammasomes, including NLRP3.[10,11] Activation of caspase induces release of pro-inflammatory factors such as interleukin-1 beta (IL-1β) and interleukin-18 (IL-18), which leads to breakdown of nuclear DNA in target cells and the formation of pores in the cell membrane.[12–14] The non-canonical pathway is mediated by caspase-11, which does not require the participation of inflammasomes.[15,16]

Recent research has revealed the involvement of the canonical pathway of pyroptosis in ALF.[17–19] Studies have found that activation of NLRP3 inflammasomes causes hepatocyte pyroptosis, liver inflammation, fibrosis,[20] and injury associated with ischemia-reperfusion,[21] heat-shock,[22] and sepsis.[23] Studies conducted in mouse models of ALF have also shown activation of NLRP3 inflammasomes, induced release of pro-inflammatory factors and aggravated liver failure.[17] However, most of the studies only focused on the canonical pathway. GSDMD protein is executioner of pyroptosis in both the canonical and non-canonical pathways; inhibition of GSDMD is thus, another potential therapeutic target for ALF. This study investigated the activation of canonical and non-canonical pyroptosis pathways and explored the role of GSDMD inhibitor necrosulfonamide (NSA) in a mouse model of ALF.

Methods

Animals

Seventy male 8-week-old specific pathogen-free (SPF)-grade C57BL/6J mice weighing 20–25 g were purchased from Shanghai SLAC Laboratory Animal Co. Ltd. The mice were raised at the Experimental Animal Center of Fujian Medical University in a controlled environment at 23–25°C, SPF-level environment, 40–60% humidity, and five mice per cage. Before the procedures, mice were adaptively reared in a 12-h light/dark cycle for 1 week, with *ad libitum* access to food and water. All procedures involving were conducted in accord with the Guide for the Care and Use of Laboratory Animals of the National Institutes of Health, and were approved by the Animal Welfare & Ethics Committee of the Fujian Medical University (no. FJMU IACUC2019-0050).

Mice were randomly assigned to four groups using a random number table: (1) A normal control group (n=10) with intraperitoneal injection of the same volume of saline as the ALF model modeling reagent; (2) An ALF group (n=20) with intraperitoneal injection of LPS (Sigma-Aldrich, Saint Louis, Missouri, USA) 50 μg/kg + D-GalN 800 mg/kg (Macklin, Shanghai, China) to establish an ALF model[24,25]; (3) A dimethyl sulfoxide (DMSO) intervention group (n=20) with intraperitoneal injection of the same amount of DMSO (Sigma-Aldrich) as the NSA group prior to establishment of the model; and (4) an NSA intervention group (n=20) with NSA (EMD Millipore, Darmstadt, Germany) dissolved in DMSO. NSA 20 mg/kg was administered by intraperitoneal injection 30 m before the establishment of the animal model.[26] A diagram the study design is shown in Supplementary Figure 1.

Survival

Survival was observed for 24 h.[27,28] Except for the control group, 10 animals in each group were randomly selected for observation of survival after modeling once every 30 m.

Serum enzyme-linked immunosorbent (ELISA) and ALT assays

Except for those observed to determine the survival rate, mice in each group were sacrificed 6 h after modeling. The eyes were removed to collect blood, which was placed in a 1.5 mL centrifuge tube, centrifuged at 4,000 rpm for 15 m, and the supernatant was removed. Serum levels of IL-1β and IL-18 were determined with ELISA kits (mlbio, Shanghai, China). Serum ALT was assayed with a FUJI NX500iVC automatic dry biochemical analyzer (FUJIFILM, Shanghai, China).

Histological analysis

After the mice were sacrificed, the liver was quickly removed and fixed in 10% formaldehyde solution for pathological sections. After paraffin embedding, hematoxylin-eosin staining (HE) was performed. Liver inflammation was evaluated by light microscopy (DM2500; Leica, Buffalo Grove, IL, USA). Two pathologists assessed liver tissue injury in a double-blind manner according to the following four parameters: structural destruction of liver lobules, hepatocyte necrosis, hepatic sinusoidal hemorrhage, and inflammatory cell infiltration. Five different randomly selected fields (400× magnification) per mouse were used for scoring. The scoring criteria were: 1=0–25%; 2=25–50%; 3=50–75%; 4=75–100%. The liver injury score was the sum of the scores for the above four parameters.[21,29] The liver injury score ranged from 4 to 16.

Table 1. qRT-PCR primer sequences

Gene	Primer	Sequence (5′–3′)
Nlrp3	Forward	CCCTTGGAGACACAGGACTC
	Reverse	GAGGCTGCAGTTGTCTAATTCC
Casp1	Forward	ACCCTCAAGTTTTGCCCTTT
	Reverse	GATCCTCCAGCAGCAACTTC
Gsdmd	Forward	CCATCGGCCTTTGAGAAAGTG
	Reverse	ACACATGAATAACGGGGTTTCC
Casp11	Forward	ACAAACACCCTGACAAACCAC
	Reverse	CACTGAGTTCAGACTTGTTAAA
Il-1β	Forward	GCCACCTTTTGACAGTGATGAG
	Reverse	CCTGAAGCTCTTGTTGATGTGC
Il-18	Forward	TCTGACATGGCAGCCATTGT
	Reverse	CAGGCCTGACATCTTCTGCAA
β-actin	Forward	GAGACCTTCAACACCCCAGC
	Reverse	ATGTCACGCACGATTTCCC

Quantitative real-time polymerase chain reaction (qRT-PCR)

Quick-RNA MicroPrep (ZYMO, Irvine, CA, U.S.A) was used to extract total RNA. Reverse transcription was performed following the instructions of Takara PrimeScript. RT Reagent Kit with gDNA Eraser (Perfect Real Time) (Takara, Beijing, China). qRT-PCR was performed with a LightCycler 96 qRT-PCR instrument (Roche, Mannheim, Germany) following the instructions included with the TB Green Premix Ex *Taq*™ (Tli RNase H Plus) (Takara) reagent. The qRT-PCR primers are shown in Table 1.

Western blotting

Protein concentration was determined with a bicinchoninic acid (BCA) protein quantification kit (ThermoFisher Scientific, Rockford, IL, USA) following to the manufacturer's instructions. After preparation of the gels, the sample was slowly added to the lane. After electrophoresis, the proteins were transferred and blocked. After blocking, the polyvinylidene difluoride (PVDF) membranes were incubated overnight with the primary antibodies anti-caspase-11 (ab180673; Abcam, Cambridge, UK), anti-GSDMD (AF4012; Affinity, Jiangsu, China), anti-caspase-1 (ab1872; Abcam), anti-NLRP3 (ab214185; Abcam), or anti-IL-1β (ab9722; Abcam). Subsequently, the membranes were incubated with the secondary antibody. Then, the membranes were exposed with a gel imager (Gel Doc2000; Bio-Rad, Hercules, CA, USA).

Statistical analysis

GraphPad Prism 8.0.1 (http://www.graphpad.com/) was used for statistical analysis. Data were reported as means±standard deviations. Between-group differences were assessed with *t*-

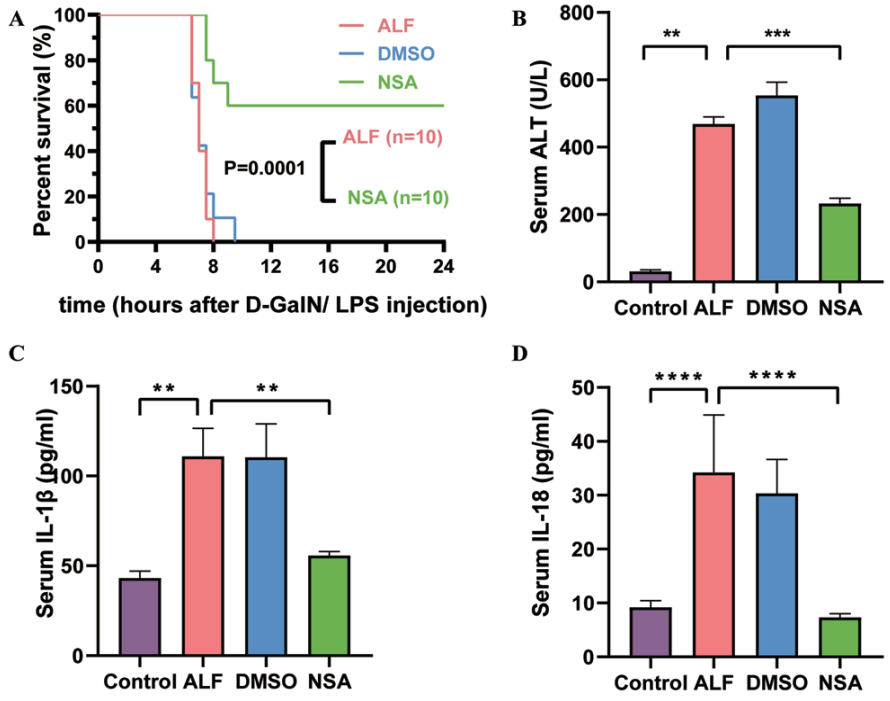

Fig. 1. (A) Survival and serum, (B) ALT, (C) IL-1β, and (D) IL-18. Data are means±standard deviations (ALT, n=3; IL-1β and IL-18, n=5). ***p*<0.01, ****p*<0.001, *****p*<0.0001. ALF, acute liver failure; ALT, alanine aminotransferase; D-GalN, D-galactosamine; DMSO, dimethyl sulfoxide; IL-1β, interleukin 1 beta; IL-18, interleukin 18; LPS, lipopolysaccharide; NSA, necrosulfonamide intervention group.

tests or Mann-Whitney tests. Comparisons of three or more groups were performed using one-way analysis of variance or non-parametric tests. Pairwise comparisons were tested by the Sidak test, Tamhane's T2 test, or Dunn's test. Survival analysis was performed by the Kaplan-Meier method, and between-group differences in survival were assessed using log-rank tests. Two-sided *p*-values <0.05 were considered significant.

Results

Effect of NSA on ALF survival

Survival curves are shown in Figure 1A. The first death in the ALF group occurred 6.5 h after modeling. Most deaths occurred at 7 h, and all animals in the ALF group died within 8 h. The survival rate in the DMSO group was similar to that in the ALF group. The first death in the NSA group occurred at 7.5 h, which was longer than that in the ALF and DMSO groups. The 24 h survival rate in the NSA group was 60%, which was significantly better than that in the ALF group (p=0.0001).

NSA alleviated liver injury in ALF mice

Six hours after establishing the ALF mice model, the mean serum ALT levels in the ALF, DMSO, and NSA groups were 468.3 U/L, 552.7 U/L, and 232 U/L, respectively. The ALT level in the NSA group was significantly lower than that in the ALF group (p<0.005; Fig. 1B). The gross pathology results, including HE staining and liver injury scores are shown in Figure 2 and Supplementary Figure 2. There were no signs of liver injury in the control group (Fig. 2). On gross examination, livers of the ALF and DMSO groups were dark red, relatively swollen, and had scattered bleeding points on the surface. Histopathologically, massive necrosis and hepatic sinusoidal hemorrhage were found in both the ALF and DMSO groups. Both ALF and DMSO groups showed predominant inflammatory cell infiltration. The NSA intervention significantly reduced the liver damage, scores that were significantly lower than those in the ALF group (p<0.005; Supplementary Fig. 2).

NSA reduced the expression of the inflammatory cytokines in ALF mice

The ELISA results are shown in Figure 1C, D. Serum IL-1β and IL-18 levels in the ALF group were higher than those in the control group (p<0.01 and p<0.001, respectively). Serum of IL-1β and IL-18 levels in the DMSO group were not significantly different from those in the ALF group. Serum IL-1β and IL-18 levels in the NSA group were significantly lower than those in the ALF group (p<0.01 and p<0.001, respectively).

Pyroptosis was activated during ALF

The transcription levels of *Casp1*, *Casp11*, and *Gsdmd* are shown in Figure 3. *Casp1* and *Casp11* mRNA expression was significantly higher in the ALF and DMSO groups than in the control group (*Casp1*, p<0.05 and *Casp11*, p<0.01). *Gsdmd* transcription was inhibited in the ALF group (p<0.05). The expression of proteins involved in the pyroptosis pathway, NLRP3, cleaved caspase-11, cleaved caspase-1, and IL-1β are shown in Figures 4 and 5. All were upregulated in the ALF group (all p<0.05). The executors of the pyroptosis pathway, GSDMD, and GSDMD-NT, were also significantly upregulated in the ALF group (both p<0.0001).

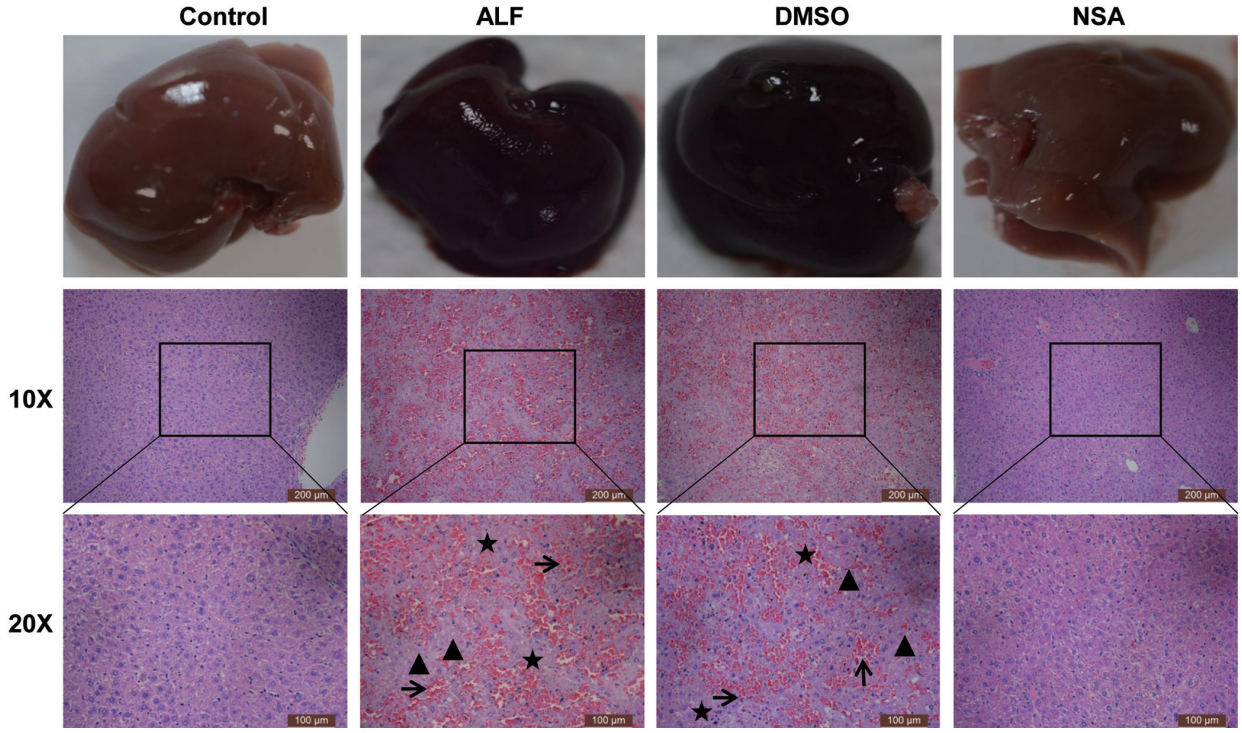

Fig. 2. Effects of NSA on liver tissue pathology in different groups. Triangles (▲) indicate hepatic structure collapse; asterisks (★) indicate hepatocyte edema and necrosis; arrows (→) indicate hepatic sinusoid hemorrhage and inflammation. ALF, acute liver failure group; Control, normal group; DMSO, dimethyl sulfoxide group; NSA, necrosulfonamide intervention group.

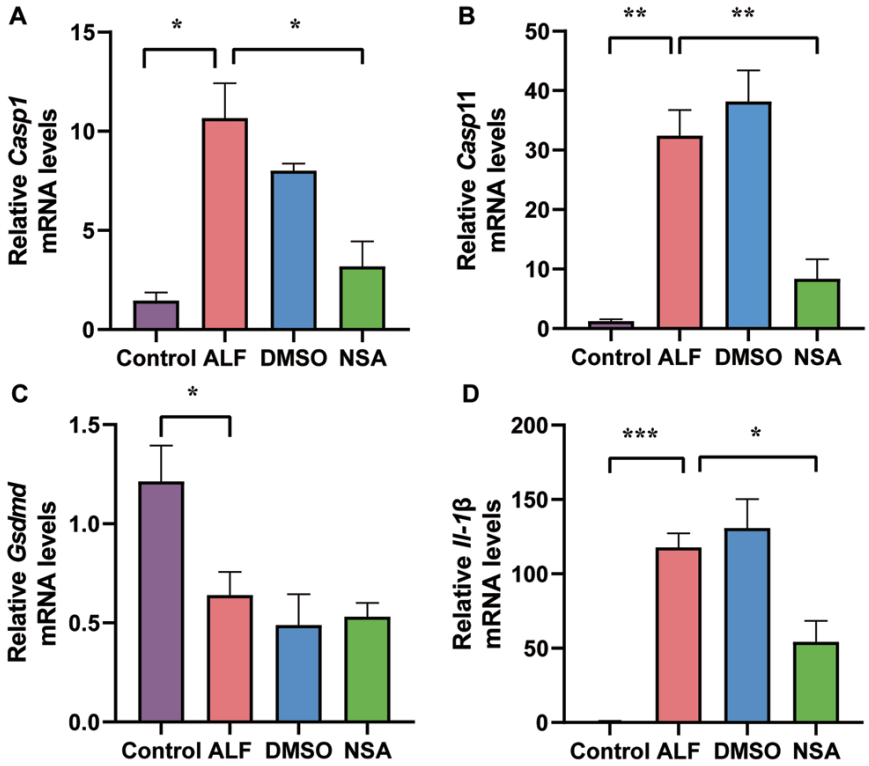

Fig. 3. Effects of NSA on mRNA levels of key molecules in the pyroptosis pathway. Expression of (A) *Casp1* mRNA; (B) *Casp11* mRNA. (NSA and DMSO, n=3; Control and ALF, n=4; (C) *Gsdmd* mRNA, n=4; (D) *Il-1β* mRNA. (NSA and DMSO, n=3; ALF, n=4; and control, n=5). Data are means±standard deviation. *p<0.05, **p<0.01, ***p<0.001, ****p<0.0001. ALF, acute liver failure; Control, normal; DMSO, dimethyl sulfoxide; NSA, necrosulfonamide.

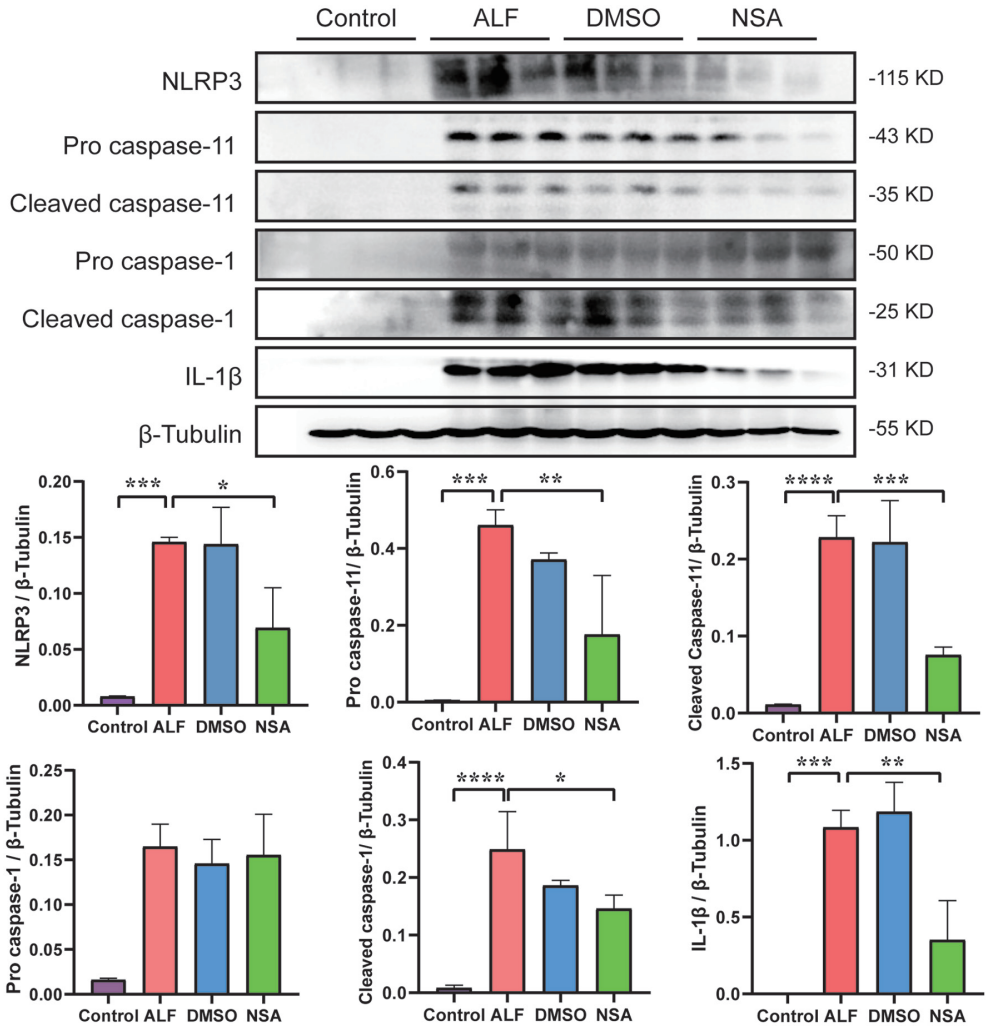

Fig. 4. Effects of NSA on key molecules in the pyroptosis pathway. (A) Western blotting of NLRP3, pro caspase-11, cleaved caspase-11, pro-caspase-1, cleaved caspase-1, and IL-1β. Relative expression of (B) NLRP3; (C) pro-caspase-11; (D) cleaved caspase-11; (E) pro-caspase-1; (F) cleaved caspase-1; and (G) IL-1β. Data are means±standard deviations (n=3). *p<0.05, **p<0.01, ***p<0.001, ****p<0.0001. ALF, acute liver failure; Control, normal; DMSO, dimethyl sulfoxide; NSA, necrosulfonamide.

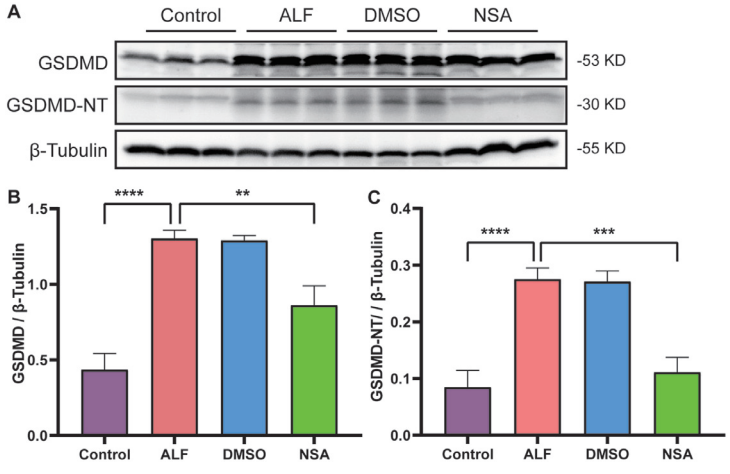

Fig. 5. Effect of NSA on GSDMD in ALF. (A) Western blotting of GSDMD and GSDMD-NT; (B) Relative expression of GSDMD and (C) GSDMD-NT. Data are means±standard deviations (n=3). **p<0.01, ***p<0.001, ****p<0.0001. ALF, acute liver failure; Control, normal; DMSO, dimethyl sulfoxide; NSA, necrosulfonamide.

NSA attenuated ALF via inhibition of the pyroptosis pathway

Casp1 and *Casp11* mRNA expression was lower in the NSA group than in the ALF group (both $p<0.05$; Fig. 3A, B). *Gsdmd* transcription was inhibited in the ALF group, and was not changed by NSA intervention (Fig. 3C). After NSA intervention, the expression of pyroptosis pathway molecules, including GSDMD, GSDMD-NT, NLRP3, cleaved caspase-1, cleaved caspase-11, and L-1β, were significantly lower than those in the ALF group (Figs. 4, 5) (GSDMD, $p<0.01$; GSDMD-NT, $p<0.001$; NLRP3, $p<0.05$; cleaved caspase-1, $p<0.05$; cleaved caspase-11, $p<0.005$; and IL-1β, $p<0.01$).

Discussion

Given that GSDMD is the common executor protein of the two pyroptosis pathways, direct inhibition of GSDMD may be useful for treating pyroptosis-related diseases. In this animal study, we observed activation of pyroptosis in ALF and revealed the potential role of NSA in ALF mice. The pyroptosis pathway was activated in the ALF mice model, and NSA inhibited the pyroptosis pathway and improved survival of ALF model mice.

NSA is a recently identified direct inhibitor of GSDMD. Rathkey *et al*.[26] were the first to report the direct binding of NSA and GSDMD in cells and mouse models of sepsis, resulting in the inhibition of GSDMD-NT oligomerization and inhibition of the formation of pyroptotic pores. Although NSA acts on human mixed lineage kinase domain-like (MLKL) protein, mouse MLKL protein has no Cys86 site, and the formation of disulfide bonds in MLKL protein is limited, resulting in NSA being unable to inhibit necrosis in mice.[26] After NSA intervention, there was significant improvement in survival time and liver injury, as shown by the serum indices and pathological findings, which suggests a potential therapeutic role of NSA in ALF.

The study results revealed activation of both canonical and non-canonical pyroptosis pathways in ALF. After NSA intervention, GSDMD, GSDMD-NT, caspase-1, caspase-11, and inflammatory cytokines were inhibited, indicating that NSA functioned via the pyroptosis pathway. We also found that an upstream molecule of the pyroptosis pathway, NLRP3, was decreased after NSA intervention. The reason may be that NSA inhibited the cascade effect of pyroptosis. Pyroptosis can be activated by damage-associated molecular patterns (DAMPs) released by injured or dead cells.[30] After NSA inhibited the GSDMD channel formation and prevented cell death, fewer DAMPs were released, which reduced the activation of NLRP3. That led to reduced potassium outflow, causing inhibition of NLRP3 activation.[31] Previous studies have also shown that NSA not only inhibits GSDMD-NT oligomerization, but also inhibits the activation of NLRP3, caspase-1, and IL-1β.[8]

Some study limitations should be acknowledged. Previous studies have demonstrated the participation of both hepatocytes and immune cells in the pyroptotic pathway.[18] Our study did not identify the functional cells in this process. Single-cell sequencing, cell coculture, and specific gene knockout may help to answer this question. Second, there may be cross-talk between different cell death pathways in ALF.[32,33] The interaction between pyroptosis and other programmed cell death was not clarified in this study, and it is worthy of further attention. Third, NSA was administered 30 m before ALF modeling. However, in clinical practice, medication is typically initiated when the patient has already developed liver failure. Whether NSA is effective in patients with liver failure needs further investigation. Moreover, the side effects of NSA are not yet known, and whether the benefits outweigh the risks in clinical application is still unknown. There is still a long way to go from bench to bedside. In summary, canonical and non-canonical pyroptosis pathways were activated in ALF mice induced by LPS/D-GalN. NSA alleviated ALF by inhibiting the pyroptosis pathway. The results provide evidence in support of possible intervention for the clinical treatment of ALF.

Funding

This study was supported by Fujian Province health education joint project (No. 2019-WJ-16), Natural Science Foundation of Fujian Province (No. 2021J01226), and Startup Fund for scientific research, Fujian Medical University (2020QH1039).

Conflict of interest

SL has been an editorial board member of *Journal of Clinical and Translational Hepatology* since 2021. The other authors have no conflict of interests related to this publication.

Author contributions

Study design (YYZ, SL), performance of experiments (YLW, WJO), analysis and interpretation of data (YLW, WJO, MZ), manuscript writing (YLW), critical revision (SL, YLW), statistical analysis (YLW, SL, MZ), critical funding (YYZ, SL, YLW), administration (YYZ, SL), and technical or material support (MZ, WJO).

Data sharing statement

The data used in support of the findings of this study are included in the article.

References

[1] European Association for the Study of the Liver. EASL Clinical Practical Guidelines on the management of acute (fulminant) liver failure. J Hepatol 2017;66(5):1047–1081. doi:10.1016/j.jhep.2016.12.003, PMID:28417882.
[2] Lin S, Chen J, Wang M, Han L, Zhang H, Dong J, *et al*. Prognostic nomogram for acute-on-chronic hepatitis B liver failure. Oncotarget 2017;8(65):109772–109782. doi:10.18632/oncotarget.21012, PMID:29312647.
[3] Reuben A, Tillman H, Fontana RJ, Davern T, McGuire B, Stravitz RT, *et al*. Outcomes in Adults With Acute Liver Failure Between 1998 and 2013: An Observational Cohort Study. Ann Intern Med 2016;164(11):724–732. doi:10.7326/M15-2211, PMID:27043883.
[4] Clària J, Stauber RE, Coenraad MJ, Moreau R, Jalan R, Pavesi M, *et al*. Systemic inflammation in decompensated cirrhosis: characterization and role in acute-on-chronic liver failure. Hepatology 2016;64(4):1249–1264. doi:10.1002/hep.28740, PMID:27483394.
[5] Triantafyllou E, Woollard KJ, McPhail MJW, Antoniades CG, Possamai LA. The Role of Monocytes and Macrophages in Acute and Acute-on-Chronic Liver Failure. Front Immunol 2018;9(2948):2948. doi:10.3389/fimmu.2018.02948, PMID:30619308.
[6] Xu B, Jiang M, Chu Y, Wang W, Chen D, Li X, *et al*. Gasdermin D plays a key role as a pyroptosis executor of non-alcoholic steatohepatitis in humans and mice. J Hepatol 2018;68(4):773–782. doi:10.1016/j.jhep.2017.11.040, PMID:29273476.
[7] Tonnus W, Linkermann A. Gasdermin D and pyroptosis in acute kidney injury. Kidney Int 2019;96(5):1061–1063. doi:10.1016/j.kint.2019.07.002, PMID:31648694.
[8] Rashidi M, Simpson DS, Hempel A, Frank D, Petrie E, Vince A, *et al*. The Pyroptotic Cell Death Effector Gasdermin D Is Activated by Gout-Associated Uric Acid Crystals but Is Dispensable for Cell Death and IL-1beta Release. J Immunol 2019;203(3):736–748. doi:10.4049/jimmunol.1900228, PMID:31209100.
[9] Orning P, Lien E, Fitzgerald KA. Gasdermins and their role in immunity and inflammation. J Exp Med 2019;216(11):2453–2465. doi:10.1084/jem.20190545, PMID:31548300.
[10] Martinon F, Burns K, Tschopp J. The inflammasome: a molecular platform triggering activation of inflammatory caspases and processing of proIL-

beta. Mol Cell 2002;10(2):417–426. doi:10.1016/s1097-2765(02)00599-3, PMID:12191486.
[11] Swanson KV, Deng M, Ting JP. The NLRP3 inflammasome: molecular activation and regulation to therapeutics. Nat Rev Immunol 2019;19(8):477–489. doi:10.1038/s41577-019-0165-0, PMID:31036962.
[12] Lieberman J, Wu H, Kagan JC. Gasdermin D activity in inflammation and host defense. Sci Immunol 2019;4(39):eaav1447. doi:10.1126/sciimmunol.aav1447, PMID:31492708.
[13] Aglietti RA, Dueber EC. Recent Insights into the Molecular Mechanisms Underlying Pyroptosis and Gasdermin Family Functions. Trends Immunol 2017;38(4):261–271. doi:10.1016/j.it.2017.01.003, PMID:28196749.
[14] Mantovani A, Dinarello CA, Molgora M, Garlanda C. Interleukin-1 and Related Cytokines in the Regulation of Inflammation and Immunity. Immunity 2019;50(4):778–795. doi:10.1016/j.immuni.2019.03.012, PMID:30995499.
[15] Jon A H, Daniel A P, Youssef A, Robert K E, Edward A M. Cytoplasmic LPS activates caspase-11: implications in TLR4-independent endotoxic shock. Science 2013;341(6151):1250–1253. doi:10.1126/science.1240988, PMID:24031018.
[16] Martinon F, Tschopp J. Inflammatory caspases: linking an intracellular innate immune system to autoinflammatory diseases. Cell 2004;117(5):561–574. doi:10.1016/j.cell.2004.05.004, PMID:15163405.
[17] Wang J, Ren H, Yuan X, Ma H, Shi X, Ding Y. Interleukin-10 secreted by mesenchymal stem cells attenuates acute liver failure through inhibiting pyroptosis. Hepatol Res 2018;48(3):E194–E202. doi:10.1111/hepr.12969, PMID:28833919.
[18] Wu J, Lin S, Wan B, Velani B, Zhu Y. Pyroptosis in Liver Disease: New Insights into Disease Mechanisms. Aging Dis 2019;10(5):1094–1108. doi:10.14336/AD.2019.0116, PMID:31595205.
[19] Thurston TL, Matthews SA, Jennings E, Alix E, Shao F, Shenoy AR, *et al*. Growth inhibition of cytosolic Salmonella by caspase-1 and caspase-11 precedes host cell death. Nat Commun 2016;7(1):13292. doi:10.1038/ncomms13292, PMID:27808091.
[20] Wree A, Eguchi A, McGeough MD, Pena CA, Johnson CD, Canbay A, *et al*. NLRP3 inflammasome activation results in hepatocyte pyroptosis, liver inflammation, and fibrosis in mice. Hepatology 2014;59(3):898–910. doi:10.1002/hep.26592, PMID:23813842.
[21] Dai C, Xiao X, Li D, Tun S, Wang Y, Velkov T, *et al*. Chloroquine ameliorates carbon tetrachloride-induced acute liver injury in mice via the concomitant inhibition of inflammation and induction of apoptosis. Cell Death Dis 2018;9(12):1164. doi:10.1038/s41419-018-1136-2, PMID:30478280.
[22] Geng Y, Ma Q, Liu YN, Peng N, Yuan FF, Li XG, *et al*. Heatstroke induces liver injury via IL-1beta and HMGB1-induced pyroptosis. J Hepatol 2015;63(3):622–633. doi:10.1016/j.jhep.2015.04.010, PMID:25931416.
[23] Chen YL, Xu G, Liang X, Wei J, Luo J, Chen GN, *et al*. Inhibition of hepatic cells pyroptosis attenuates CLP-induced acute liver injury. Am J Transl Res 2016;8(12):5685–5695. PMID:28078039.
[24] Pourcet B, Zecchin M, Ferri L, Beauchamp J, Sitaula S, Billon C, *et al*. Nuclear Receptor Subfamily 1 Group D Member 1 Regulates Circadian Activity of NLRP3 Inflammasome to Reduce the Severity of Fulminant Hepatitis in Mice. Gastroenterology 2018;154(5):1449–1464.e20. doi:10.1053/j.gastro.2017.12.019, PMID:29277561.
[25] Wang T, Wang Z, Yang P, Xia L, Zhou M, Wang S, *et al*. PER1 prevents excessive innate immune response during endotoxin-induced liver injury through regulation of macrophage recruitment in mice. Cell Death Dis 2016;7(4):e2176. doi:10.1038/cddis.2016.9, PMID:27054331.
[26] Rathkey JK, Zhao J, Liu Z, Chen Y, Yang J, Kondolf HC, *et al*. Chemical disruption of the pyroptotic pore-forming protein gasdermin D inhibits inflammatory cell death and sepsis. Sci Immunol 2018;3(26):eaat2738. doi:10.1126/sciimmunol.aat2738, PMID:30143556.
[27] Xing WW, Zou MJ, Liu S, Xu T, Gao J, Wang JX, *et al*. Hepatoprotective effects of IL-22 on fulminant hepatic failure induced by d-galactosamine and lipopolysaccharide in mice. Cytokine 2011;56(2):174–179. doi:10.1016/j.cyto.2011.07.022, PMID:21843953.
[28] Kim SJ, Lee SM. NLRP3 inflammasome activation in D-galactosamine and lipopolysaccharide-induced acute liver failure: role of heme oxygenase-1. Free Radic Biol Med 2013;65:997–1004. doi:10.1016/j.freeradbiomed.2013.08.178, PMID:23994575.
[29] Baranova IN, Souza AC, Bocharov AV, Vishnyakova TG, Hu X, Vaisman BL, *et al*. Human SR-BI and SR-BII Potentiate Lipopolysaccharide-Induced Inflammation and Acute Liver and Kidney Injury in Mice. J Immunol 2016;196(7):3135–3147. doi:10.4049/jimmunol.1501709, PMID:26936883.
[30] Anderton H, Wicks IP, Silke J. Cell death in chronic inflammation: breaking the cycle to treat rheumatic disease. Nat Rev Rheumatol 2020;16(9):496–513. doi:10.1038/s41584-020-0455-8, PMID:32641743.
[31] Xue Y, Enosi Tuipulotu D, Tan WH, Kay C, Man SM. Emerging Activators and Regulators of Inflammasomes and Pyroptosis. Trends Immunol 2019;40(11):1035–1052. doi:10.1016/j.it.2019.09.005, PMID:31662274.
[32] Doerflinger M, Deng Y, Whitney P, Salvamoser R, Engel S, Kueh AJ, *et al*. Flexible Usage and Interconnectivity of Diverse Cell Death Pathways Protect against Intracellular Infection. Immunity 2020;53(3):533–547.e537. doi:10.1016/j.immuni.2020.07.004, PMID:32735843.
[33] Kesavardhana S, Malireddi RKS, Kanneganti TD. Caspases in Cell Death, Inflammation, and Pyroptosis. Annu Rev Immunol 2020;38:567–595. doi:10.1146/annurev-immunol-073119-095439, PMID:32017655.